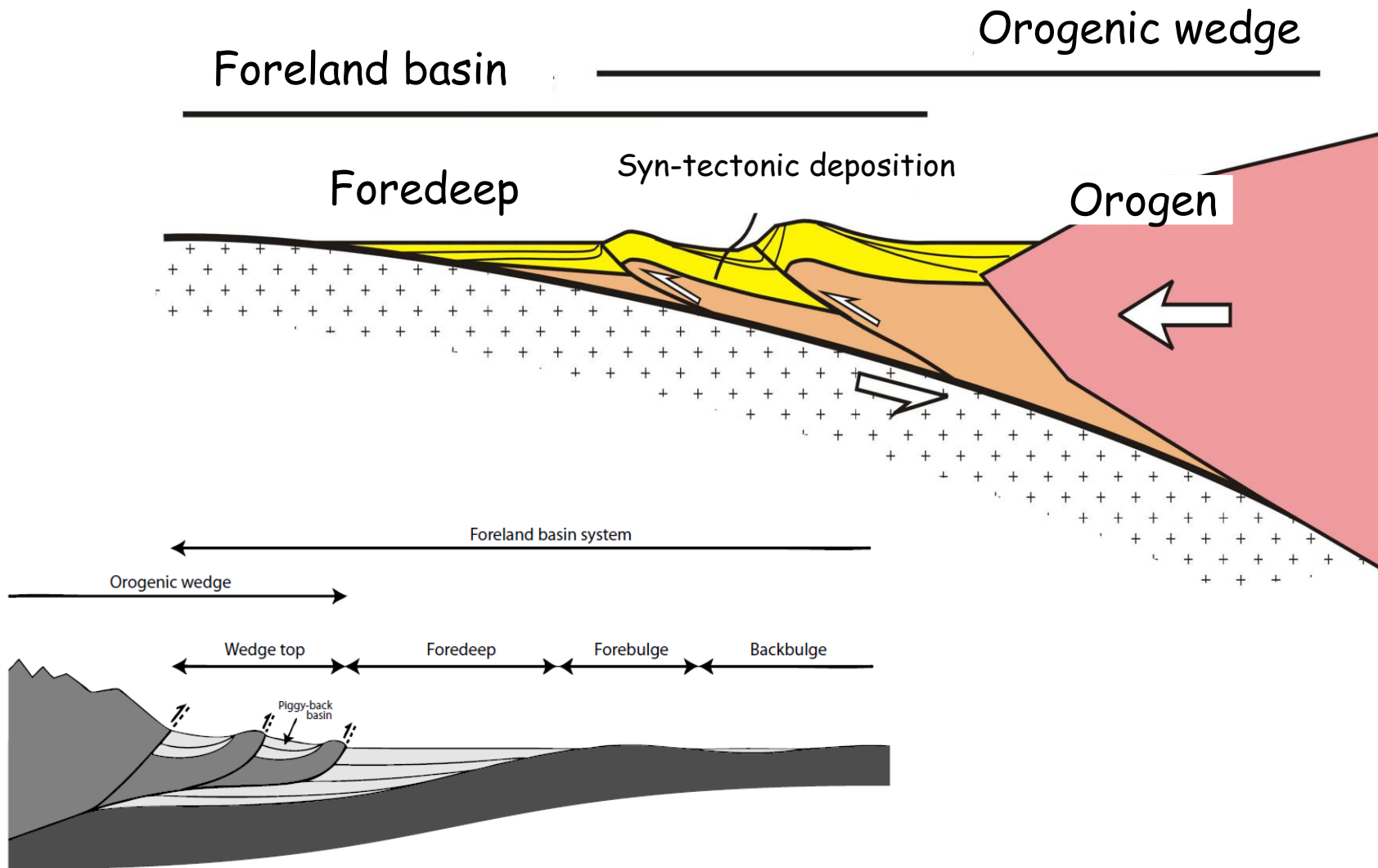


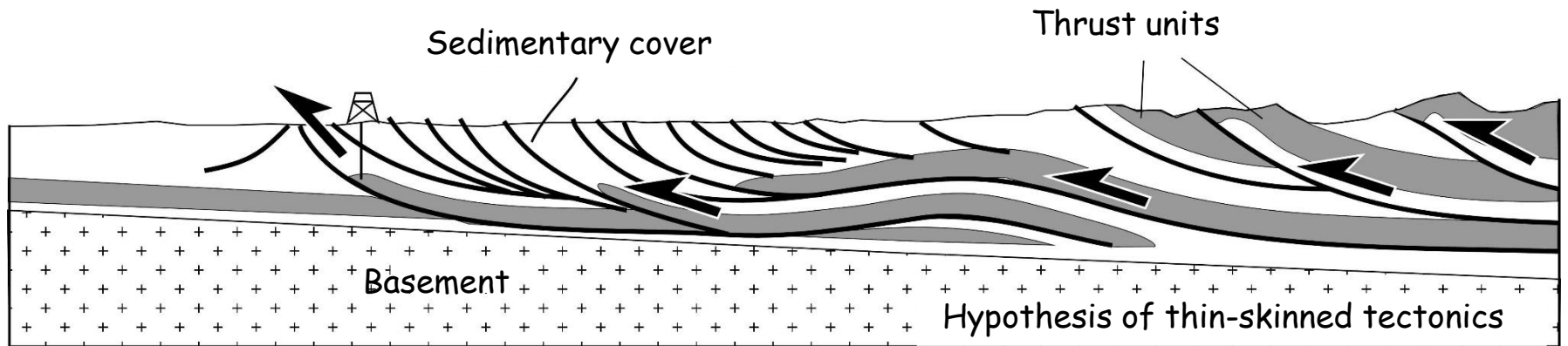
The critical-tapered wedge theory and its application to fold-and-thrust belts

Olivier LACOMBE



The fold-and-thrust belt / foreland system

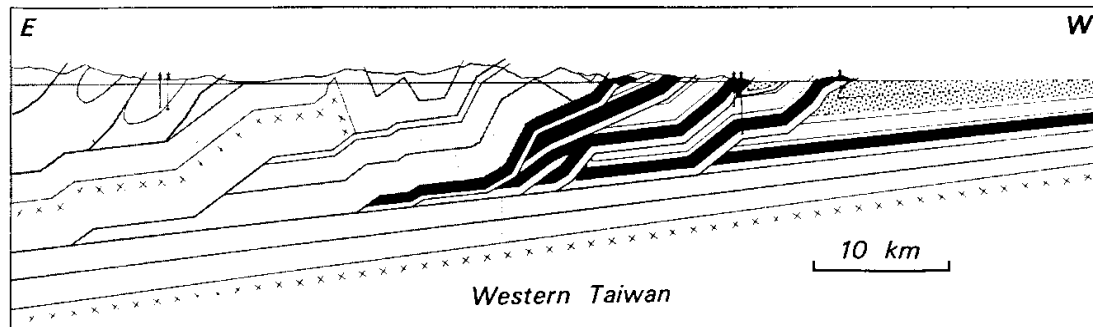
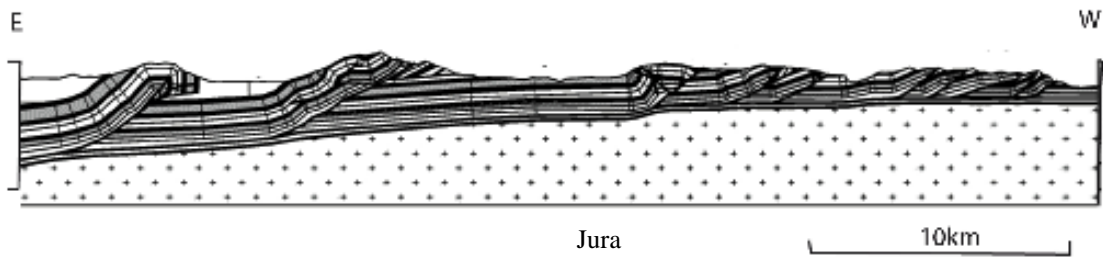
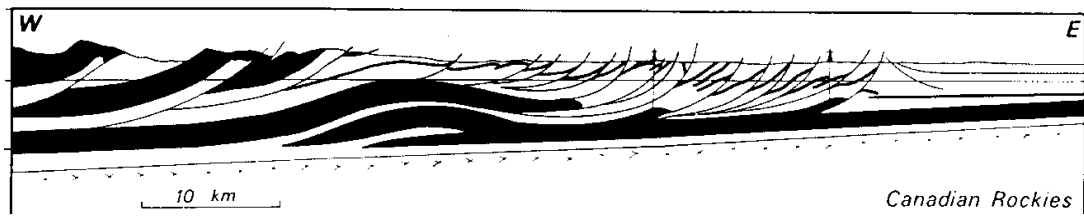


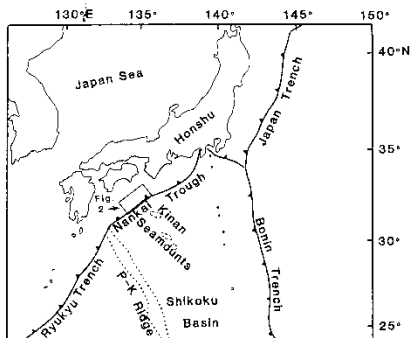
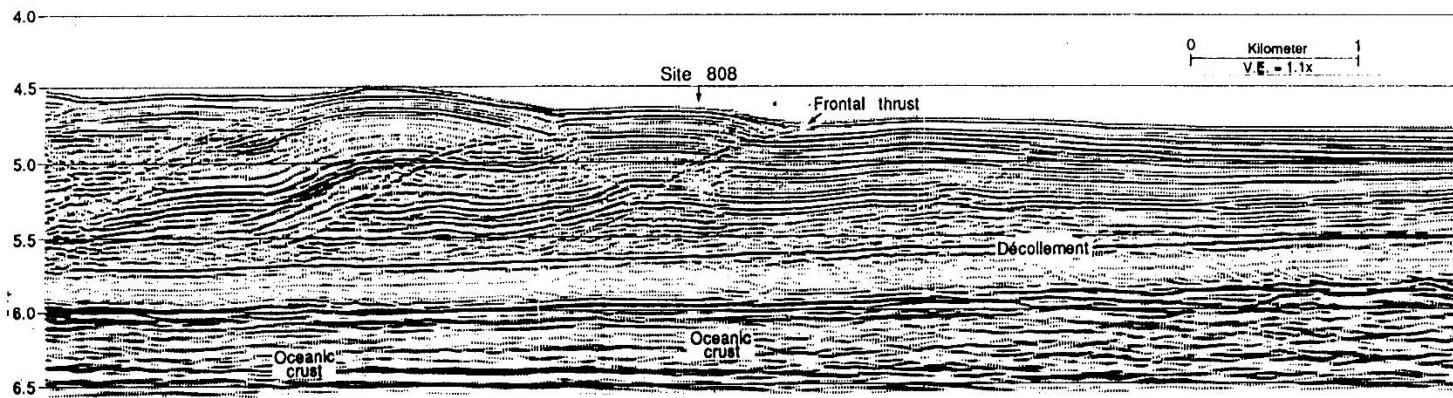


Shortening is accommodated in the upper part of the crust above a basal décollement dipping toward the hinterland

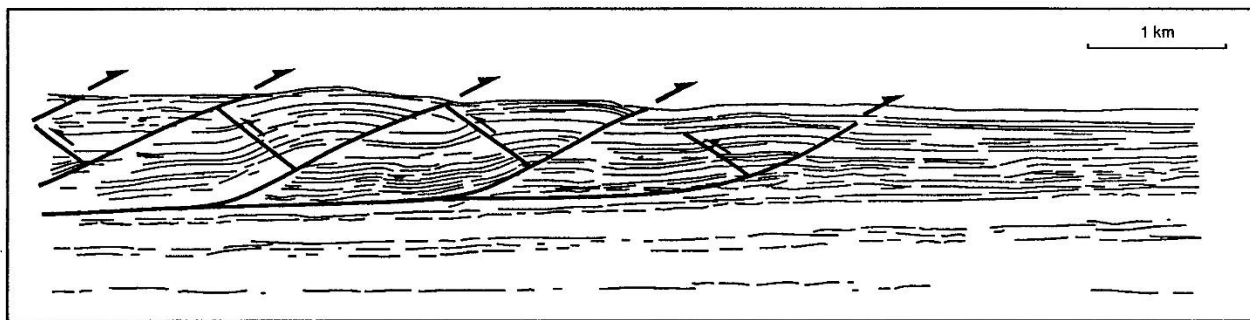
Implicit assumption of « thin-skinned » tectonic style

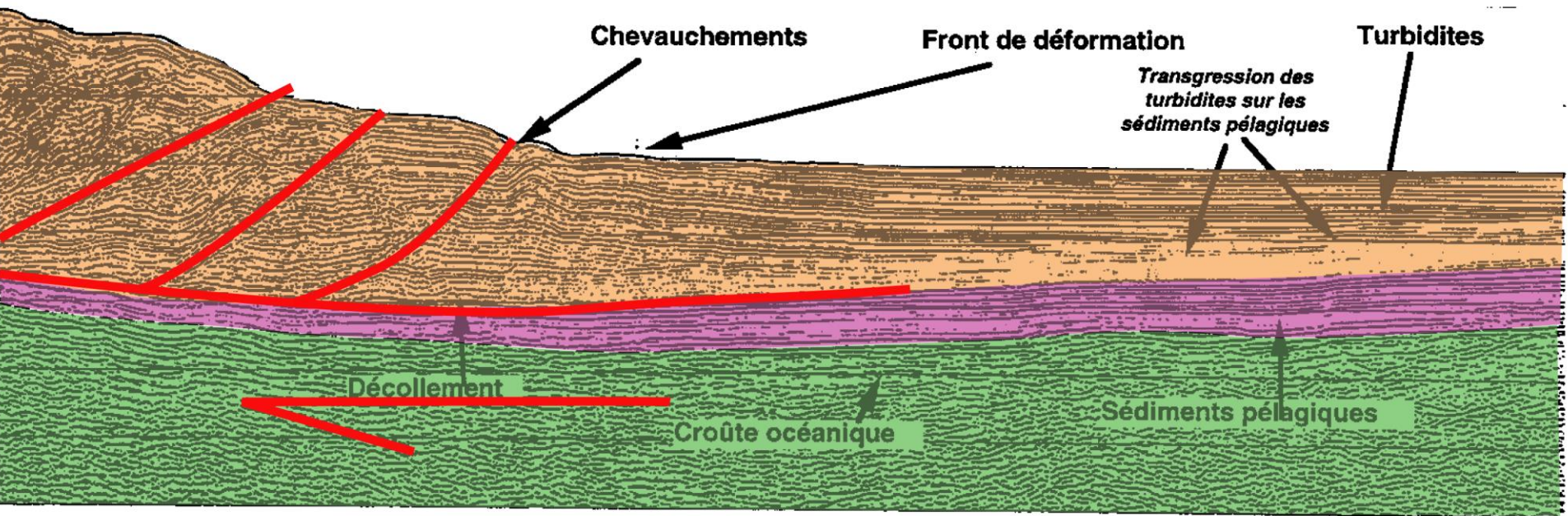
Topographic slope and dip of basal décollement define the orogenic wedge



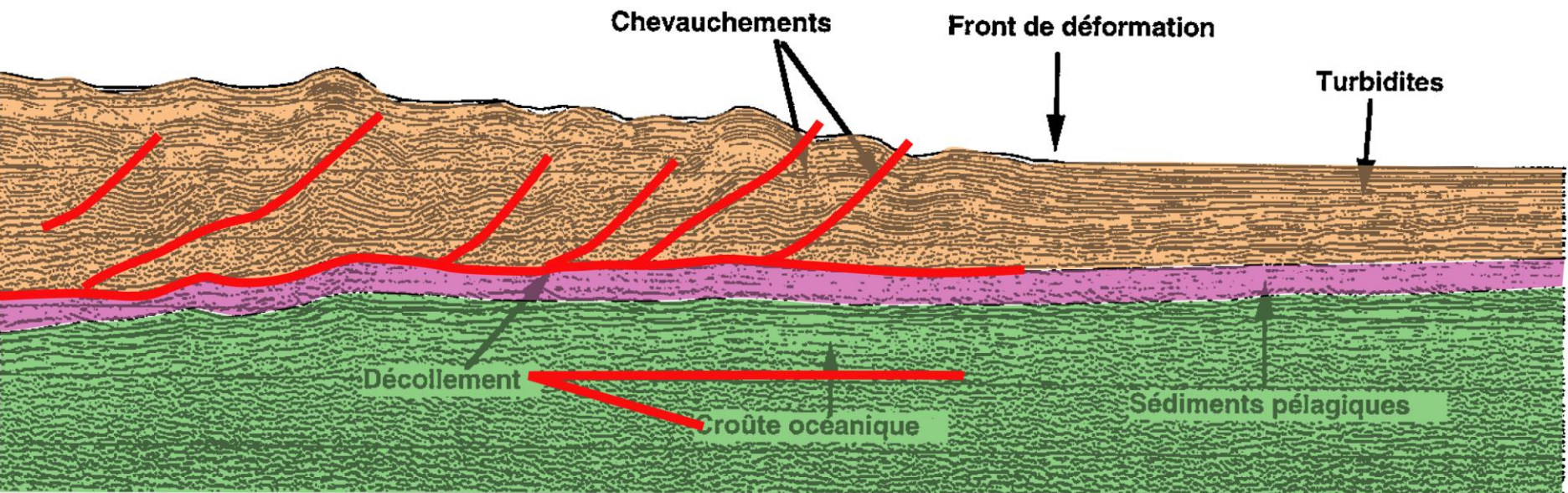


Regional tectonic map showing setting of the Nankai Trough study area (box labeled as Figure 2).





1 km



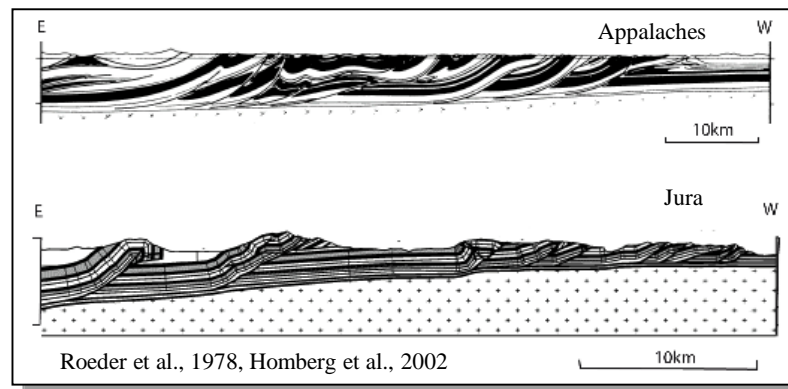
Mechanics of thin-skinned fold-and-thrust belts

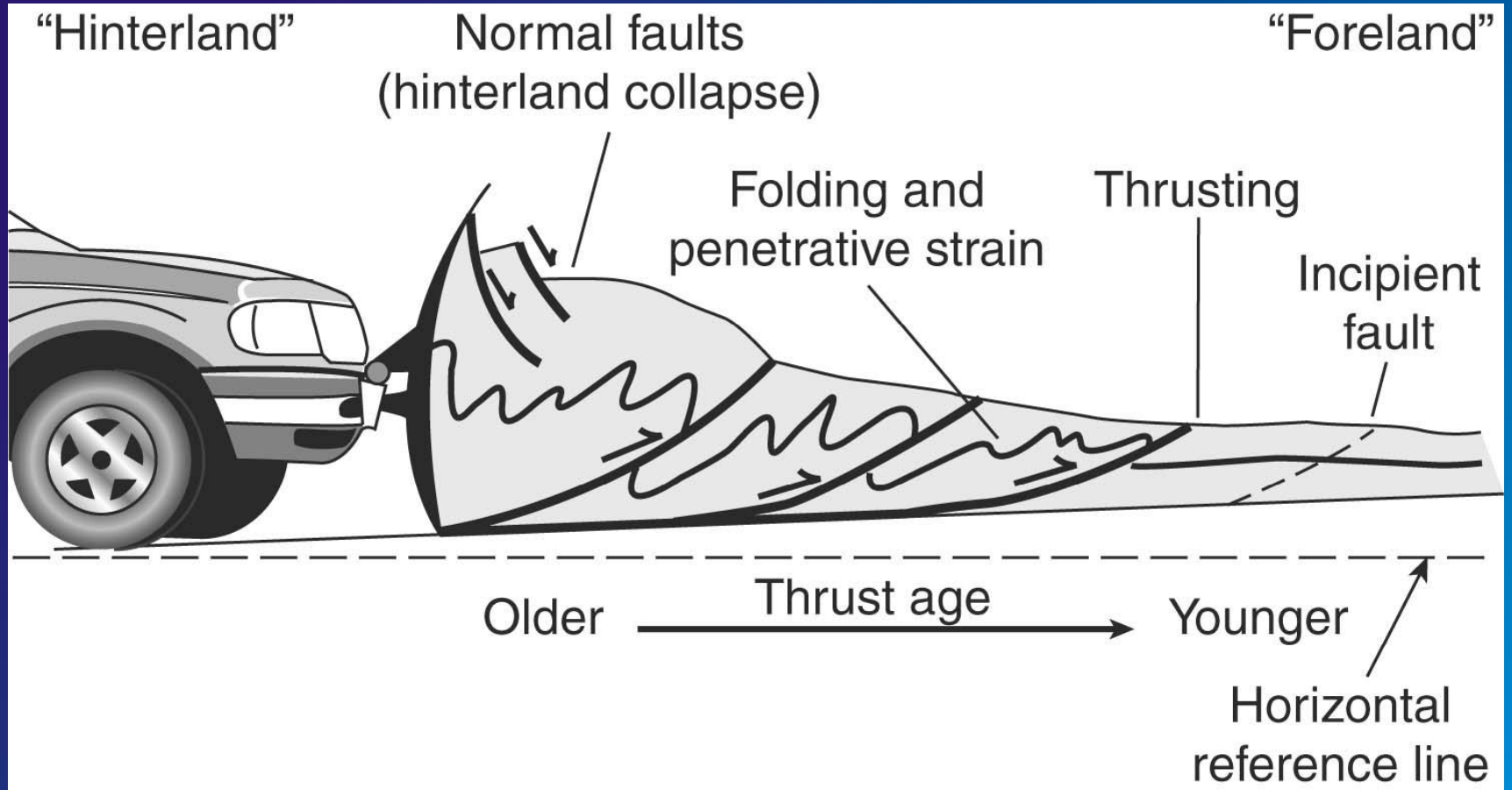
WILLIAM M. CHAPPLE *Department of Geological Sciences, Brown University, Providence, Rhode Island*

1978 : Chapple :
Wedge-shaped
concept, based
on field
observations

The essential characteristics of thin-skinned fold-and-thrust belts include the following: a wedge-shaped deforming region, thicker at the back end from which the thrusts come; a weak layer at the base of the wedge; and large amounts of shortening and thickening within the wedge. All these characteristics are incorporated into an analytical model of a perfectly plastic wedge, underlain by a weak basal layer and yielding in compressive flow.

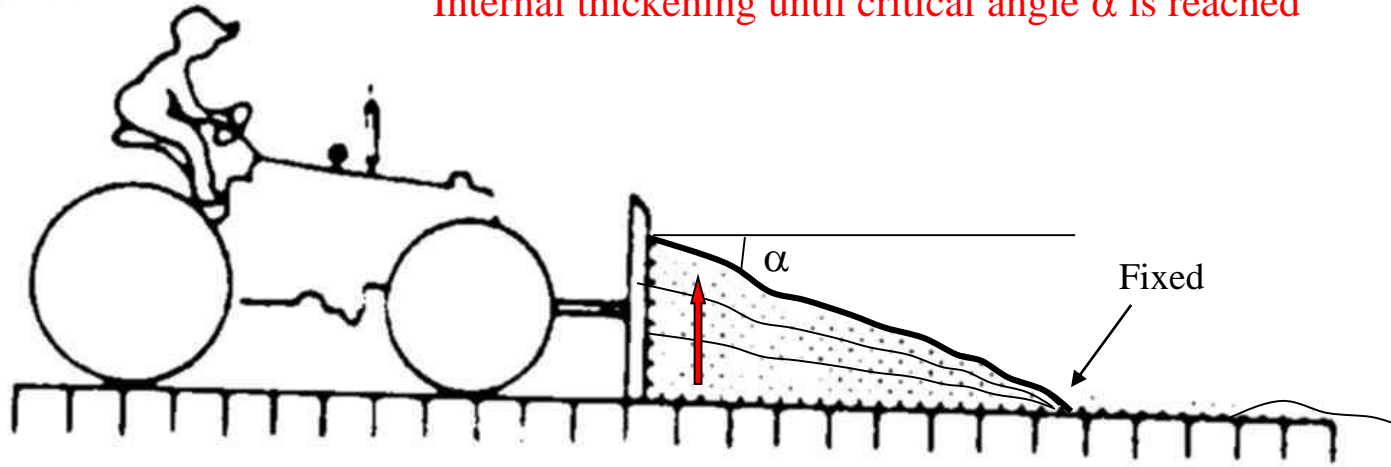
Wedge dues to
horizontal
compression, no
need to appeal
for gravity.



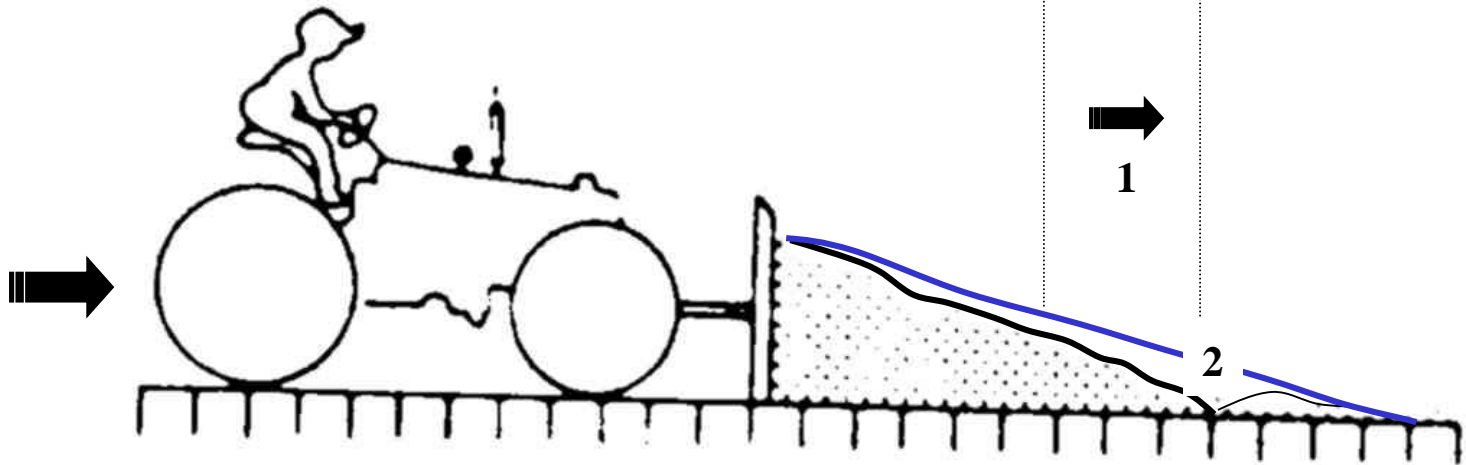




Internal thickening until critical angle α is reached



1. Basal sliding without internal thickening, then
2. New snow is incorporated in the wedge, α is lowered, then
3. The wedge will deform internally until α is reached again, and so on



The critical Taper

1983 : Davis et al. : Mechanics of wedge analogue to soil or snow in front of a moving bulldozer.

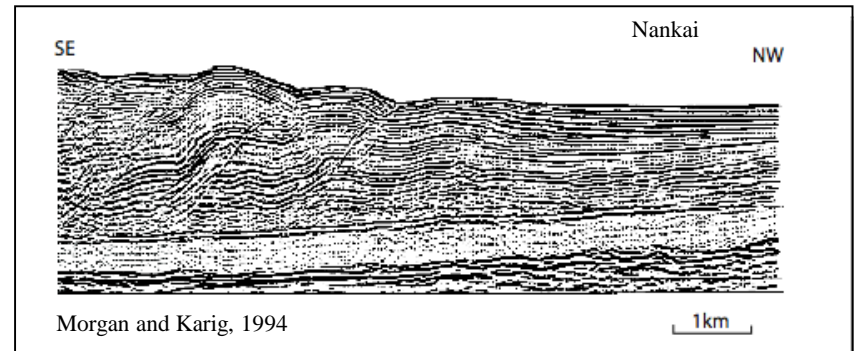
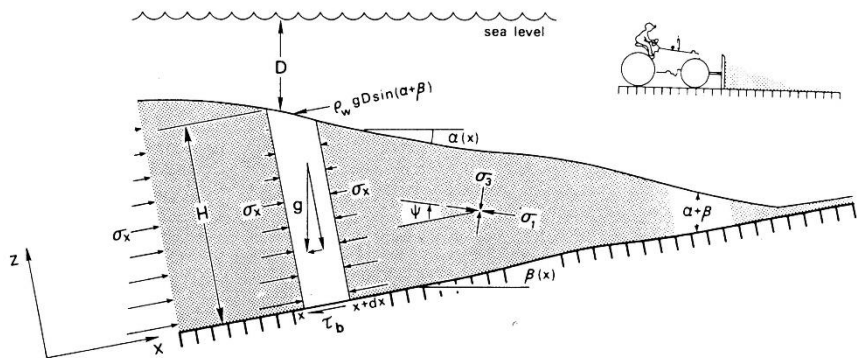
Mechanics of Fold-and-Thrust Belts and Accretionary Wedges

DAN DAVIS

Department of Earth and Planetary Sciences, Massachusetts Institute of Technology
Cambridge, Massachusetts 02139

JOHN SUPPE AND F. A. DAHLEN

The overall mechanics of fold-and-thrust belts and accretionary wedges along compressive plate boundaries is considered to be analogous to that of a wedge of soil or snow in front of a moving bulldozer. The material within the wedge deforms until a critical taper is attained, after which it slides stably, continuing to grow at constant taper as additional material is encountered at the toe. The critical taper is the shape for which the wedge is on the verge of failure under horizontal compression everywhere, including the basal decollement. A wedge of less than critical taper will not slide when pushed but will deform internally, steepening its surface slope until the critical taper is attained. Common silicate sediments and rocks in the upper 10–15 km of the crust have pressure-dependent brittle compressive strengths which can be approximately represented by the empirical Coulomb failure criterion, modified to account for the weakening effects of pore fluid pressure.



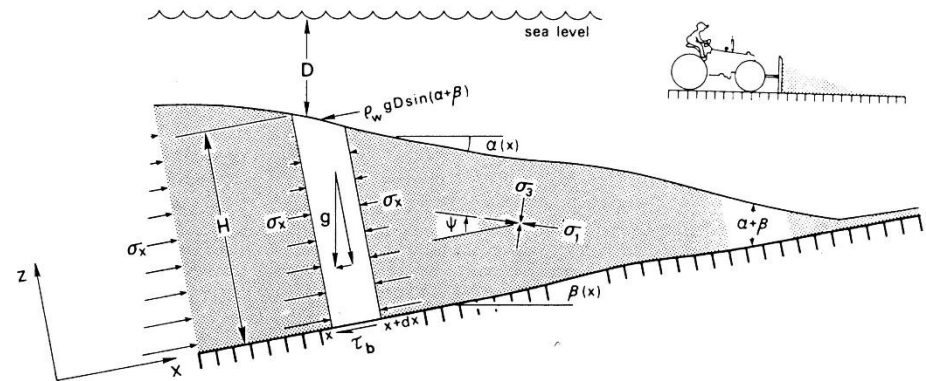
The critical Taper

Coulomb criterion : Rock deformation in the upper lithosphere is governed by pressure dependent and time independent coulomb behavior ie by **brittle fracture** (Paterson, 1978) or **frictional sliding** (Byerlee, 1978).

$$|\tau| = S_0 + \mu(\sigma_n - p_f)$$

$$\sigma_n^* = \sigma_n - p_f$$

$$|\tau| = \mu\sigma_n^*$$



Force equilibrium : Gravitational body force, pressure of water, frictional resistance to sliding along the basal decollement, compressive push :

$$\rho g H \sin \beta + \rho_w g D \sin (\alpha + \beta) + \tau_b + \frac{d}{dx} \int_0^H \sigma_x dz = 0$$

Thin-skinned structures allow small angles approximations :

$$\rho g H \beta + \rho_w g D (\alpha + \beta) + \tau_b + \frac{d}{dx} \int_0^H \sigma_x dz = 0$$

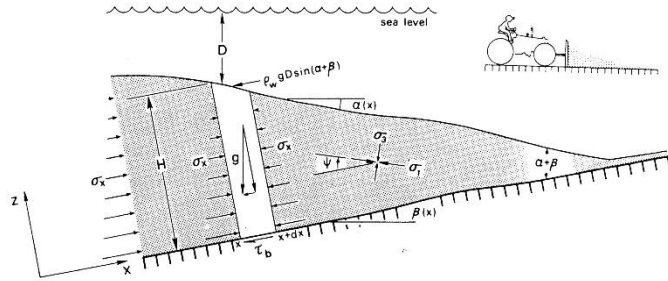
Weight of sedimentary column (lithostatic pressure)

Weight of water column

Basal frictional shear strength

Sum of lateral push forces

The critical Taper



$$\rho_w g H \beta + \rho_w g D (\alpha + \beta) + \tau_b + \frac{d}{dx} \int_0^H \sigma_x dz = 0$$

$$\int_0^H \sigma_x dz = \rho_w g D H + \frac{1}{2} \rho_w g H^2$$

$$+ 2\rho_w g \int_0^H \frac{(1-\lambda)(H-z)}{\csc \phi \sec 2\psi - 1} dz \quad (13)$$

Invoking the small-angle approximation once again, we set

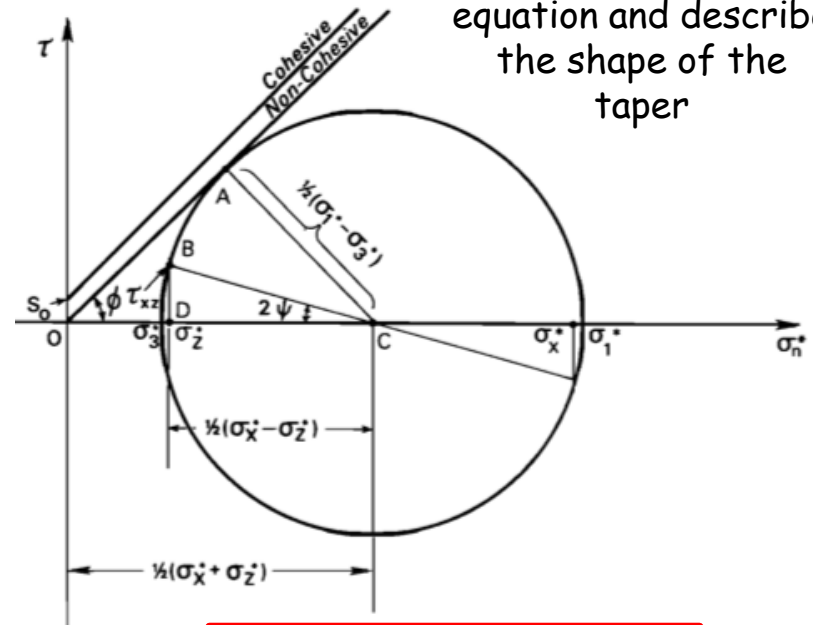
$$dH/dx = -(\alpha + \beta) \quad (14)$$

$$dD/dx = \alpha \quad (15)$$

$$K = 2H^{-1} \int_0^H \frac{dz}{\csc \phi \sec 2\psi(z) - 1}$$

$$\lambda = \frac{p_f - \rho_w g D}{|\sigma_z| - \rho_w g D}$$

The Mohr diagram is used to solve the equation and describe the shape of the taper



$$\alpha + \beta = \frac{(1 - \lambda_b)\mu_b + (1 - \rho_w/\rho)\beta}{(1 - \rho_w/\rho) + (1 - \lambda)K} \quad (18)$$

It is noteworthy that this equation contains no explicit dependence on x so that a wedge with uniform properties and a planar base should have a constant surface slope. Note, in addition, that in the limit $\lambda_b \rightarrow \lambda \rightarrow 1$, (18) reduces to $\alpha \rightarrow 0$, which is the expected result for a wedge composed of material having negligible strength.

No length scale : scale independent

The critical Taper

Sandbox validation :



Formula for dry and cohesionless sand :

$$\alpha + \beta = \frac{\mu_b + \beta}{1 + K}$$

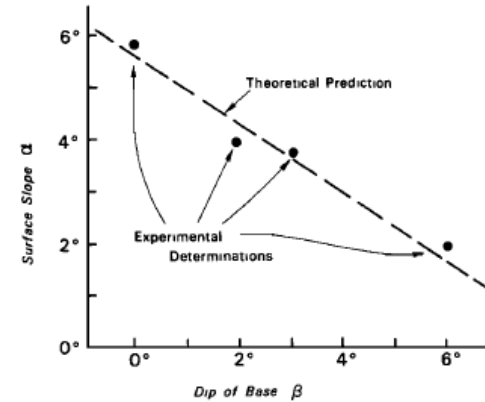
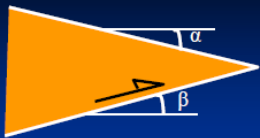


Fig. 8. Mean surface slope measured by linear regression off photographs versus dip of rigid base in sandbox experiments. Dots represent the average of eight experimental runs at $\beta = 0^\circ$, two at $\beta = 2^\circ$, fourteen at $\beta = 3^\circ$, and nine at $\beta = 6^\circ$. Line is theoretical prediction $\alpha = 5.9^\circ - 0.66\beta$.



$$\alpha + \beta = f(\mu, \mu_b, \lambda)$$

where $\lambda = \frac{p_f - \rho_w g D}{\sigma_z - \rho_w g D}$ and μ = coefficient of friction (μ_b = basal coef.)

$$\alpha + R\beta = F$$

Linear relationship between α and β

L'équilibre des forces peut se résumer à une relation linéaire:

$$F = \alpha + \beta R$$

$$\text{Où: } R = \frac{(1 - \lambda)K}{(1 - \rho_w / \rho) + (1 - \lambda)K}$$

$$F = \frac{(1 - \lambda_b)\mu_b}{(1 - \rho_w / \rho) + (1 - \lambda)K}$$

Conditions de fracturation et état critique

Dans le prisme

➔ **Critère de néorupture (Mohr-Coulomb)**

$$\tau_i = C_o + \mu_c \sigma_n$$

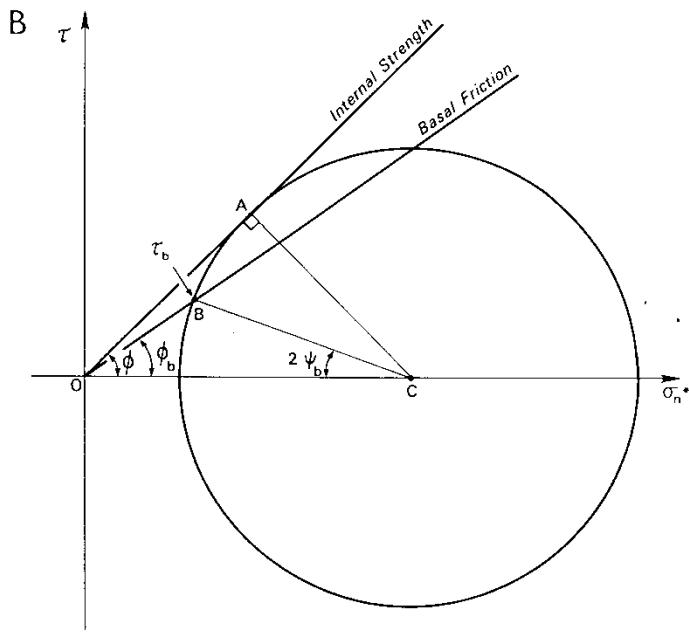
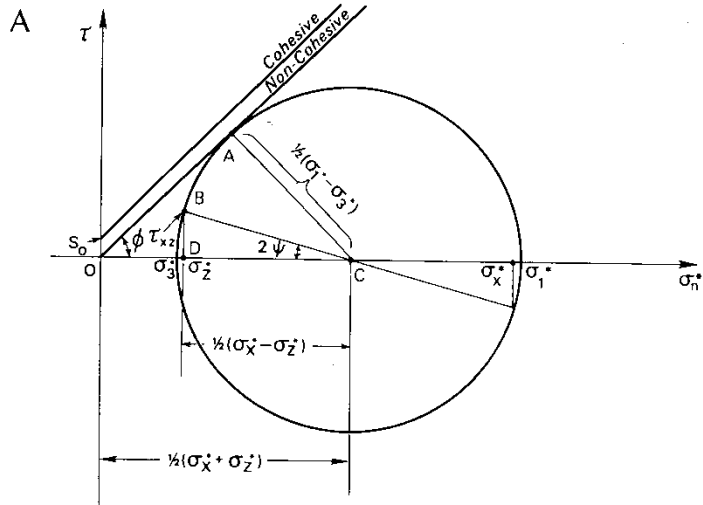
$$\tau_b = C_f + \mu_f \sigma_n$$

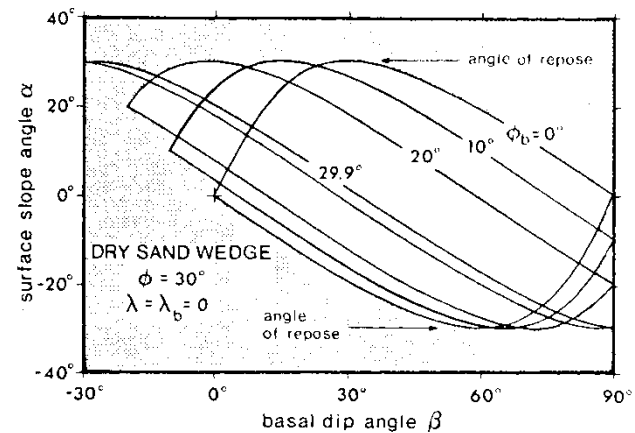
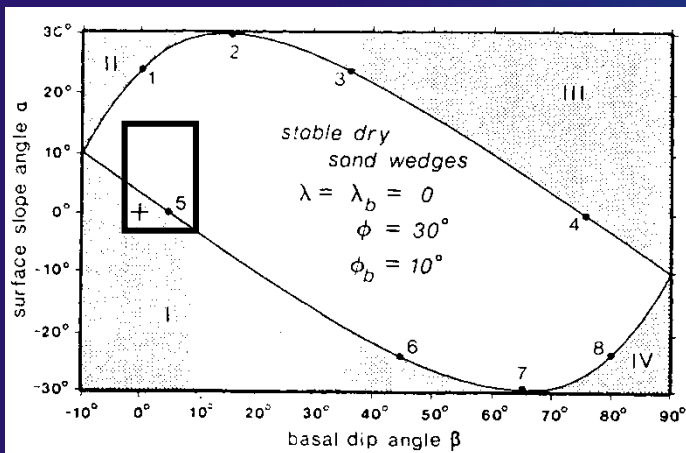
$$\text{avec } \mu_f < \mu_c$$

Le prisme est à l'état critique lorsque le cercle tangente la droite de néorupture

Base du prisme

➔ **Critère de friction**



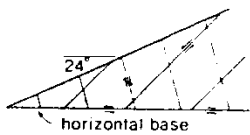


The area inside the "lens shape" corresponds to the stability regime of the wedge, when it does not deform.

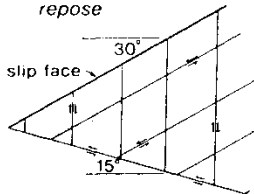
Along the envelope of the lens, the wedge is under critical conditions and is growing self-similarly. Outside of the lens, the wedge is in an under- or overcritical state. In the undercritical domain, compression is favoured, whereas extension occurs in the overcritical domain. Both types of adjustment tend to occur to restore the stability slope of the prism.

EXAMPLES OF CRITICAL DRY SAND WEDGES

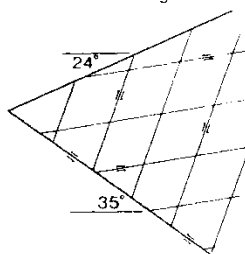
1. normal faulting and downslope flow



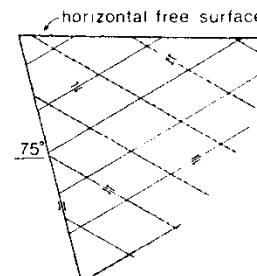
2. surface at angle of repose



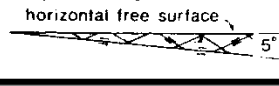
3. combined normal and thrust faulting



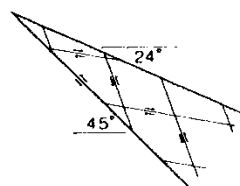
4. thrust faulting



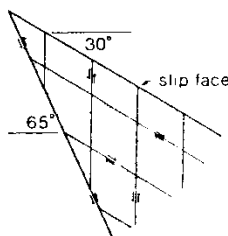
5. accretionary wedge fails by thrusting



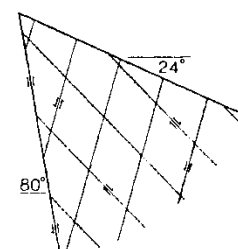
6. combined normal and thrust faulting



7. surface at angle of repose



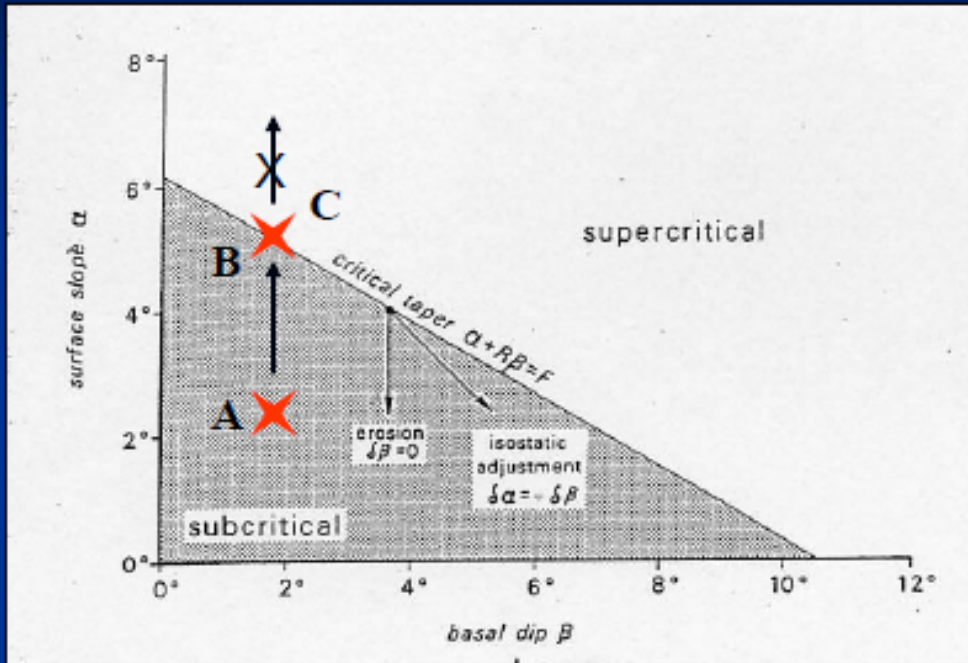
8. normal faulting



I, II, III and IV : unstable wedge.
 I and III : the undercritical wedge has to shorten by thrusting to reach equilibrium; II and IV : the overcritical wedge has to extend by normal faulting to reach equilibrium

The stability domain is large for a weak basal friction and is reduced to a line when the basal friction equals the internal friction.

Modification of the equilibrium



Example: mountain building

A: subcritical / “stable” $\rightarrow \alpha$ can increase.

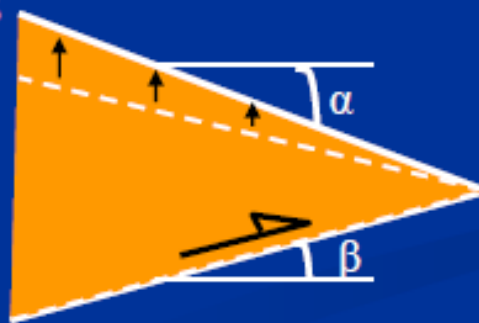
B: critical taper. α cannot increase anymore. If $\alpha >$ critical value, the taper becomes supercritical / unstable and collapses.

C: to carry on growing, the taper cannot steepen anymore so it has to “expand” horizontally as well as vertically.

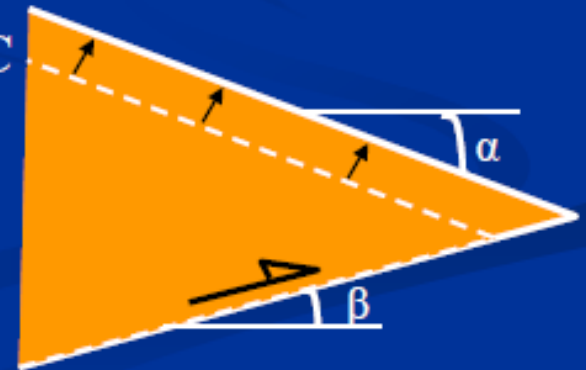
A

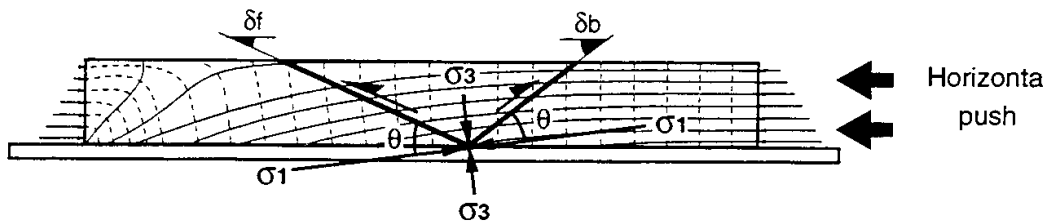
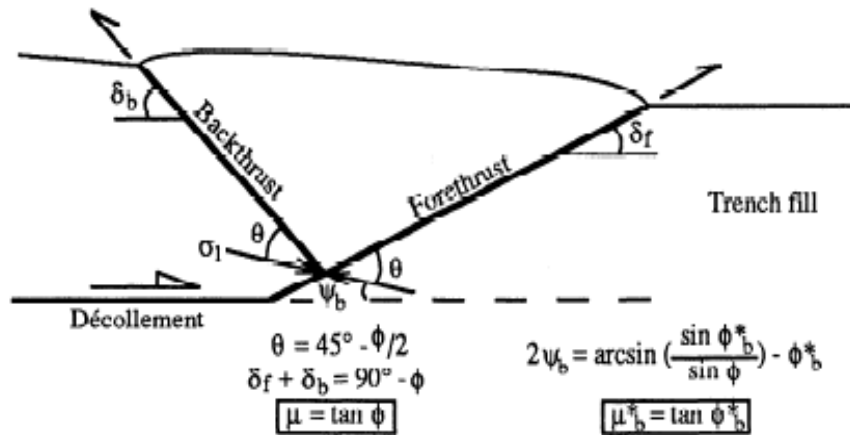


B



C

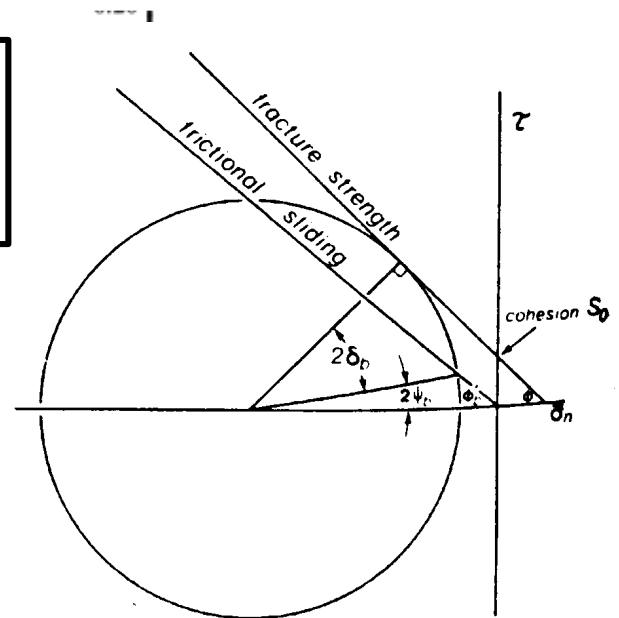
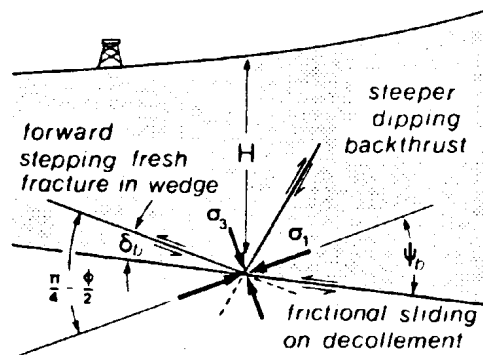




La pente des chevauchements est plus forte pour les prismes à faible friction

Les rétrochevauchements sont plus fréquents dans les prismes à faible friction basale

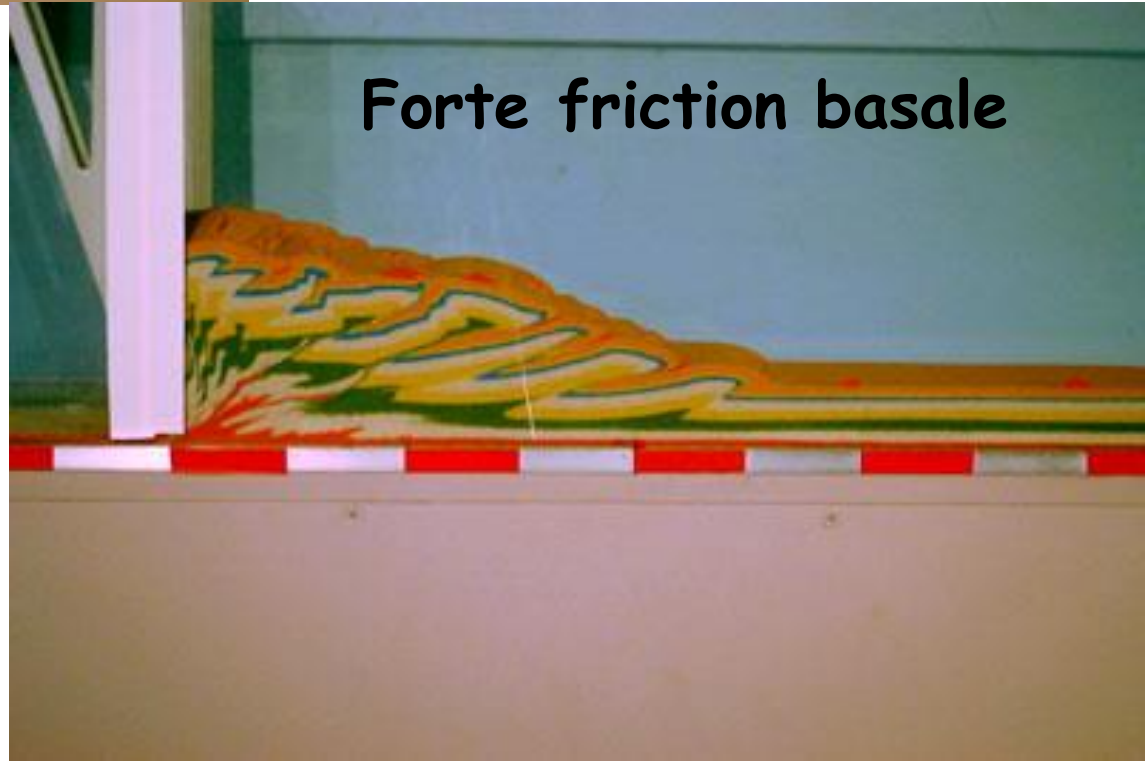
Dans la théorie du prisme de Coulomb, l'angle de la contrainte principale (ψ) est dépendant de la friction



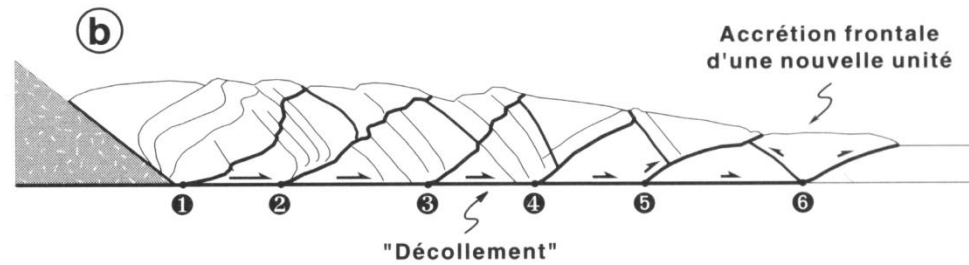
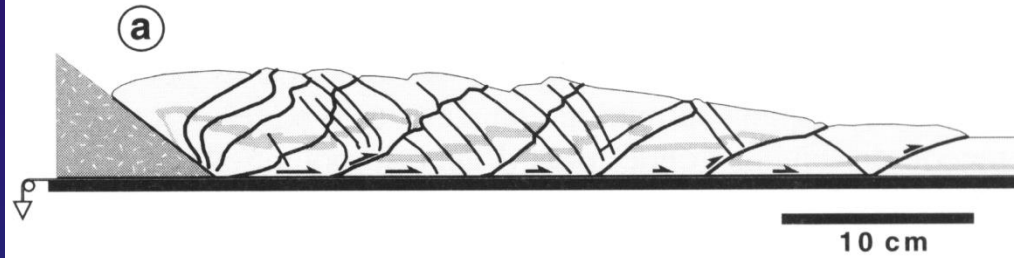
Faible friction basale



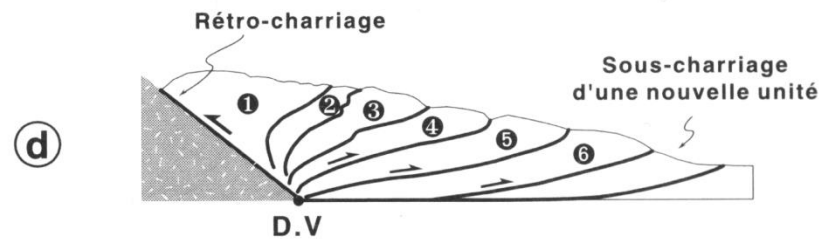
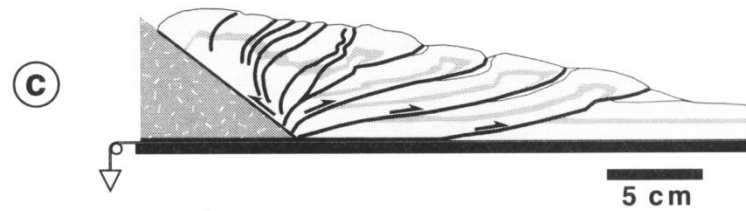
Forte friction basale



FAIBLE FRICTION BASALE



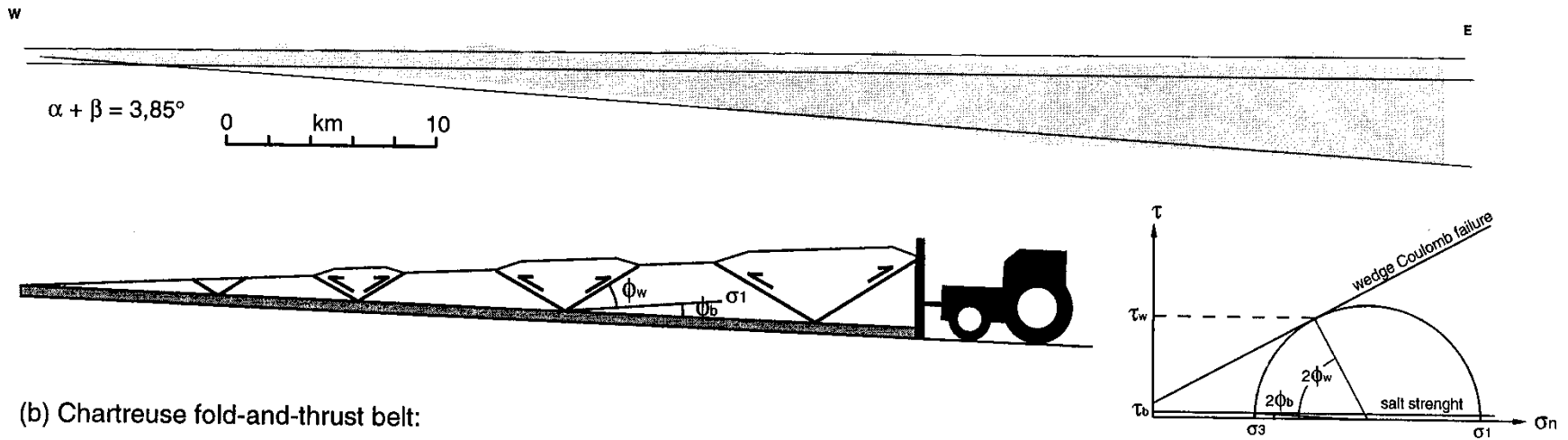
FORTE FRICTION BASALE



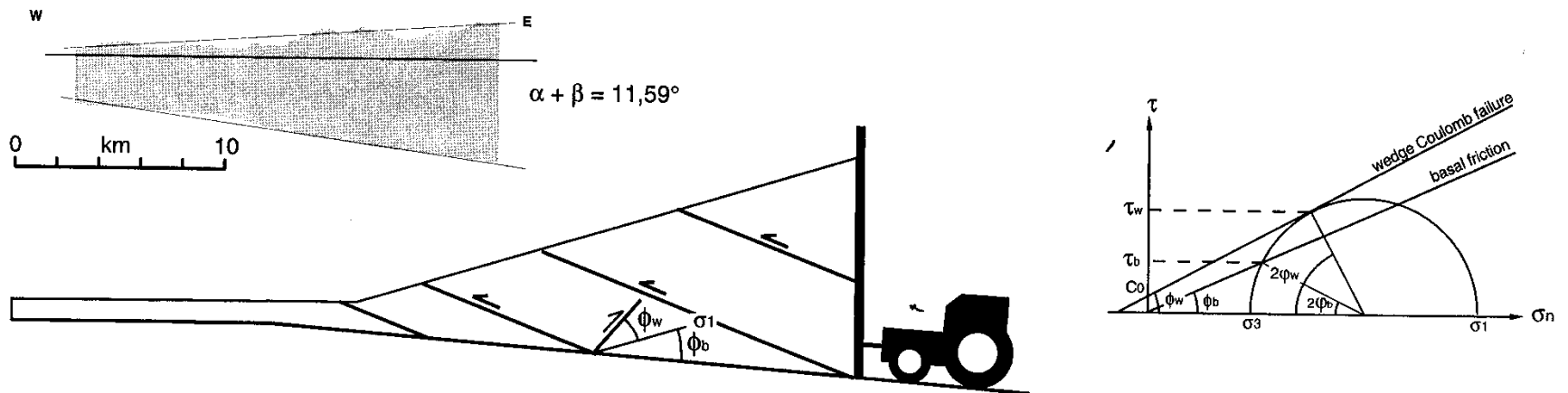
Interprétation Jura (ou Vercors)/Chartreuse en termes de prisme critique (rôle de la friction basale)

(a) Jura fold-and-thrust belt and Molasse Basin: / Vercors

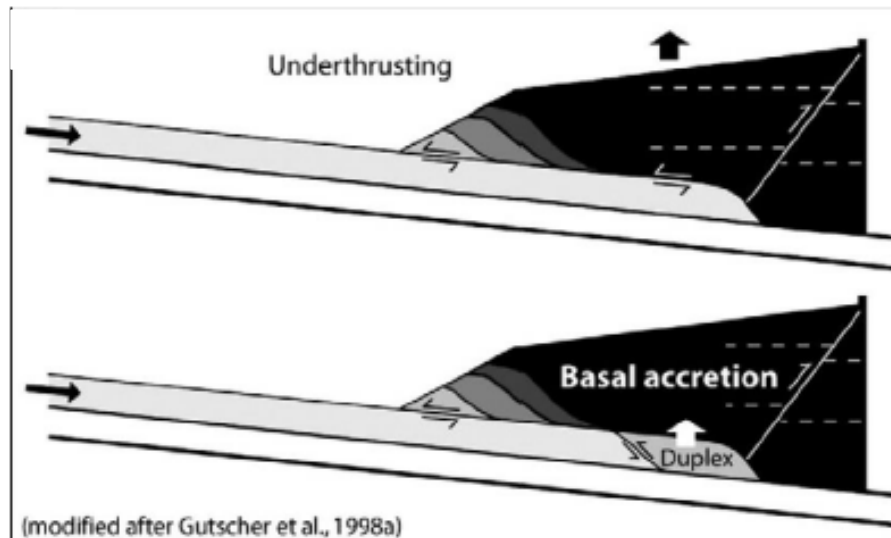
(Philippe, 1995)



(b) Chartreuse fold-and-thrust belt:



An alternative
to frontal
accretion :
basal accretion
- underplating

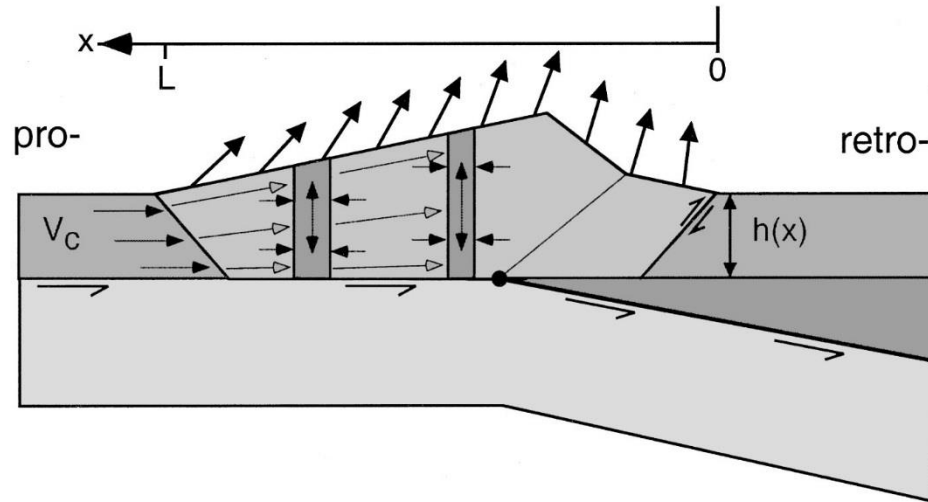


Accrétion tectonique basale

- Le sous-placage a lieu lorsque le taper du prisme est faible
- Implique le sous-charriage d'une longue unité
- Le taper du prisme augmente au cours du sous-charriage
- La friction sur le décollement intra-prisme est plus importante que sur le décollement basal : le couplage modifie la pente et la topographie de la partie supérieure du prisme
- Basculement vers des conditions d'accrétion frontale lorsque le taper est devenu trop élevé

➔ **Cyclicité sous-placage/accrétion frontale**

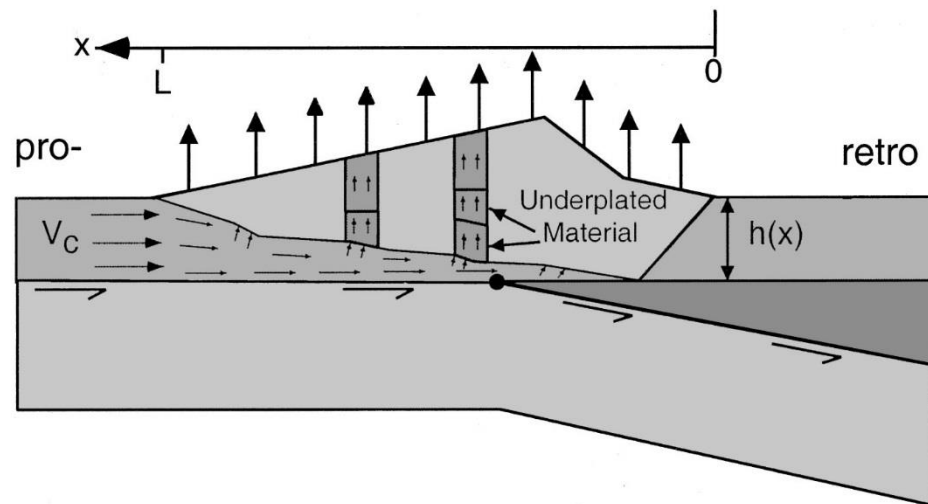
A. Frontal Accretion



End-member kinematic models of orogenic wedge growth.

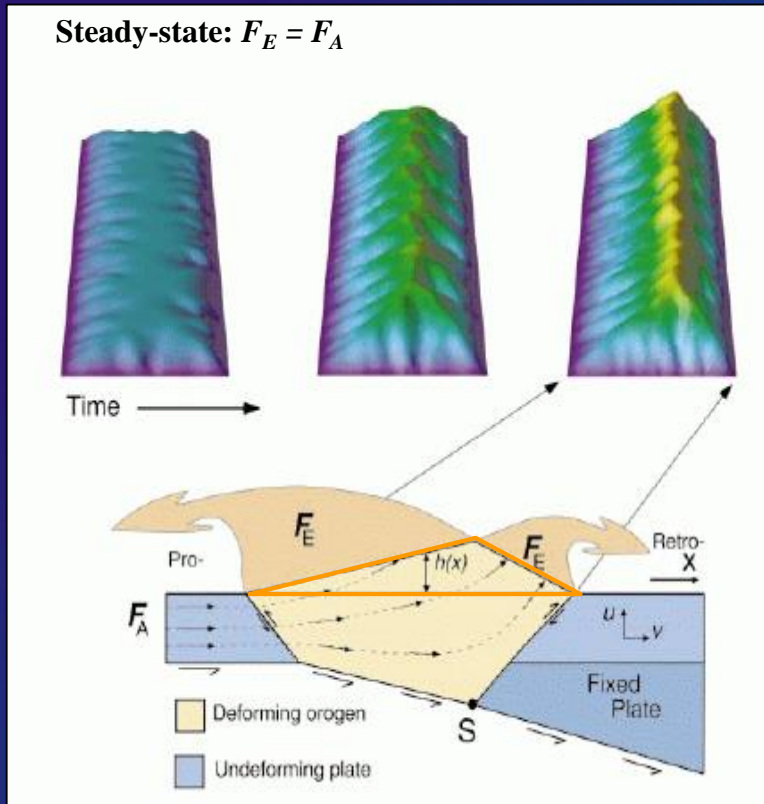
A) Frontal accretion. Wedge shortens such that a vertical column extends vertically and shortens horizontally. Vertical component of surface velocity is relatively constant.

B. Underplating



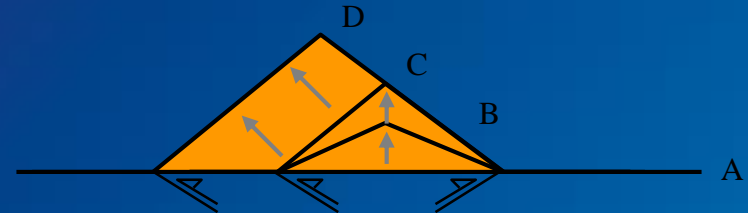
B) Underplating. Wedge does not shorten horizontally and thus has no horizontal velocity. Columns of rock move vertically at a constant rate in response to addition of new material at the base of the wedge.

Erosion controls the geometry of mountains



Willett & Brandon, Geology, 2002

F_A = flux of material accreted,
 F_E = flux of material eroded.

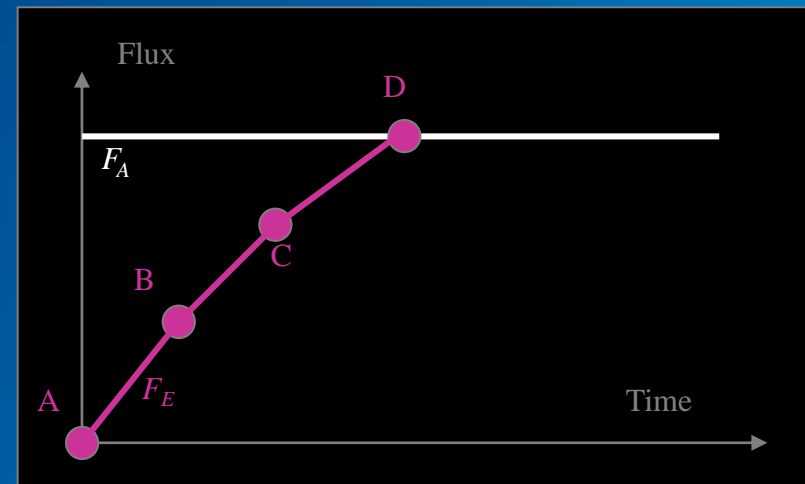


A: no topography, $F_E = 0$.

B: mountain grows → F_E increases.

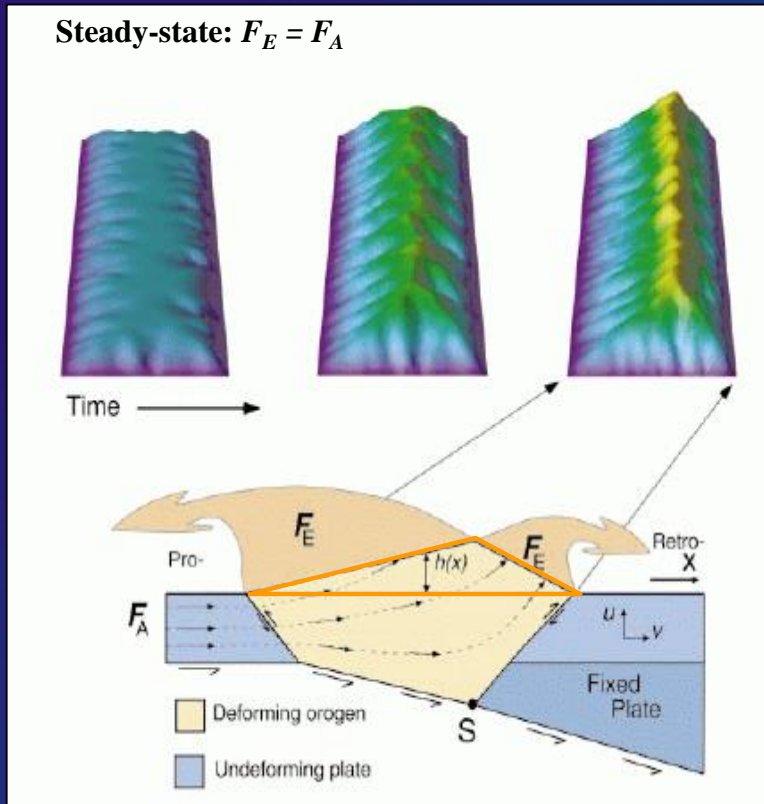
C: critical taper stage, slope α cannot increase anymore.

D: $F_A = F_E$ → steady-state. The topography does not evolve anymore.



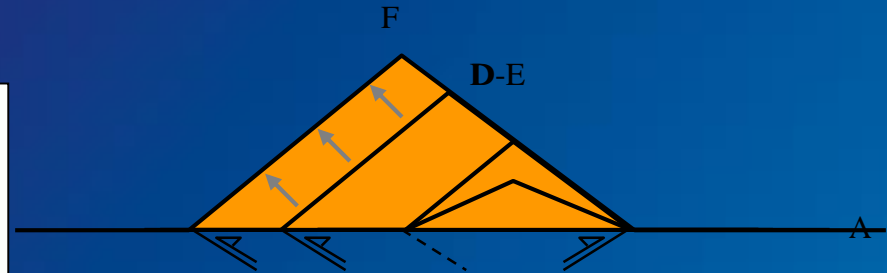
Acknowledgements : Mikaël ATTAL

Erosion controls the geometry of mountains



Willett & Brandon, *Geology*, 2002

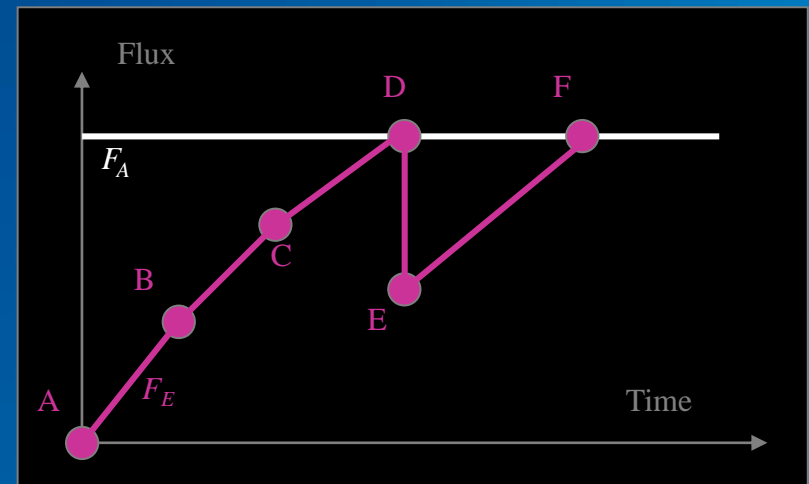
F_A = flux of material accreted,
 F_E = flux of material eroded.



D: $F_A = F_E \rightarrow$ steady-state.

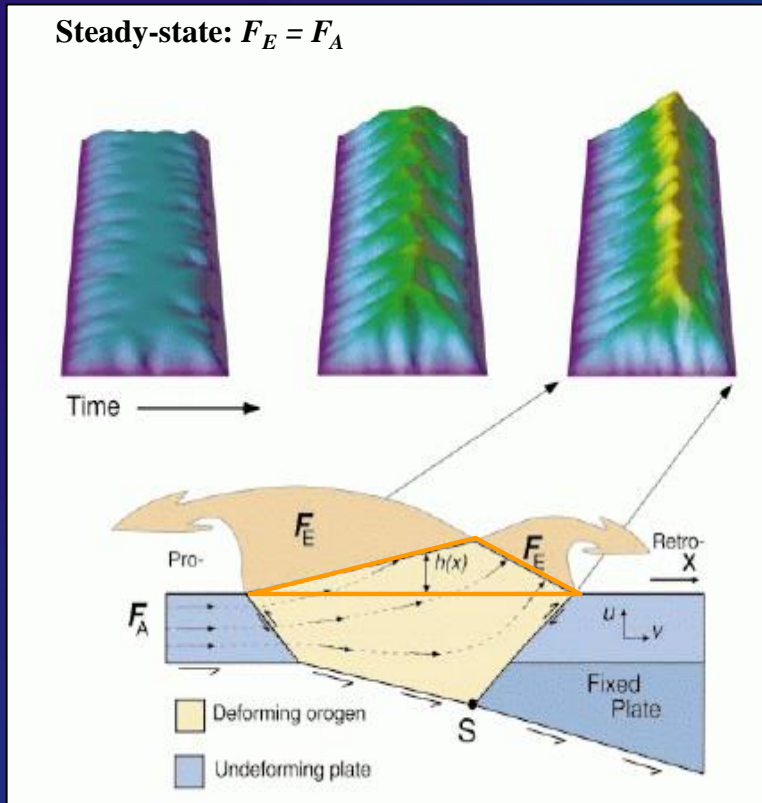
E: drop in F_E (e.g., climate change with less rain) \rightarrow erosion rate decreases \rightarrow the topography is not at steady-state anymore.

F: mountain grows again $\rightarrow F_E$ increases until a new steady-state is reached ($F_A = F_E$)



Acknowledgements : Mikaël ATTAL

Erosion controls the geometry of mountains



However, “real” mountains are more complex:

- presence of discontinuities (e.g. faults),
- different lithologies (more resistant in the core of the range),
- change in crust rheology (e.g. lower crust partially molten under Tibet → no basal friction).

Willett & Brandon, Geology, 2002

F_A = flux of material accreted,
 F_E = flux of material eroded.

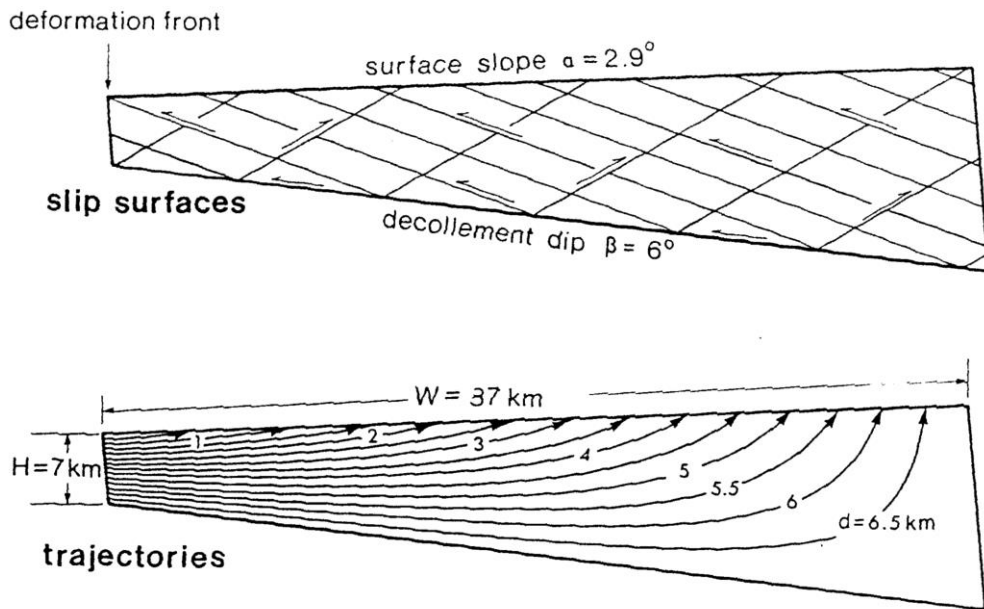


Figure 14. Theoretical slip surfaces and rock trajectories in the critically tapered Taiwan wedge, assuming $\mu = 0.85$.

Dahlen et Suppe, 1988

Willett et al., 1993

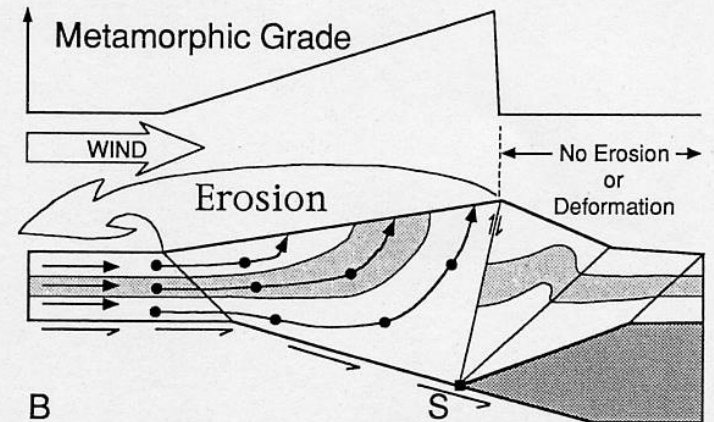
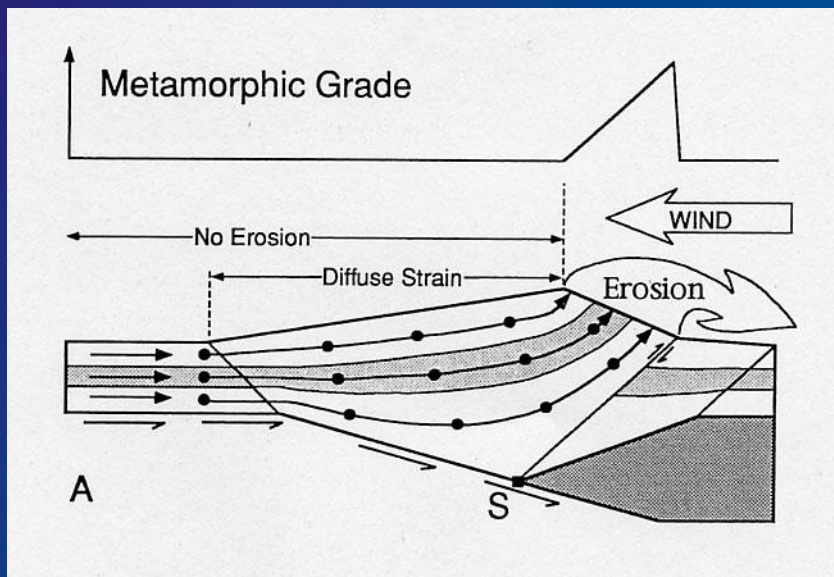


Figure 4. Effect of steady-state (constant geometry and mass) erosion and denudation. A: Retro-wedge denudation. B: Pro-wedge denudation. Passive shaded layer shows exhumed position of middle crust. Lines are material trajectories; dots are progressive equal-time positions of points initially aligned vertically. Schematic metamorphic grade is for surface rocks assuming initial equilibrium conditions.